

Passivation , Repassivation and Metastable pitting Of Bare and Surface Treated 316L stainless implant In Hank Solution

Subir Paul* and Nisha Prasad

Department of Metallurgical and Material Engineering
Jadavpur University, Kolkata-700032, India

* Principle & communicating author dr_Subir_paul@yahoo.co.in

Abstract

Passivity , its stability and breakdown, leading to localized corrosion such as pitting is the most important phenomenon for austenitic stainless steel in vivo solution. Because growth of it helps to aggravate other forms of corrosion, leading to failure of implant material. All pits , once initiated may not grow. Many of initiated pits are metastable and may be healed by repassivation. Only those of metastable pits which find favorable conditions grow into stable pits. Studies of repassivation and formation and life of metastable pits have been investigated by cyclic polarization and current transients at different fixed potential within passive. Pits were generated by passing anodic currents within passive region and the characteristic studies repassivation leading to death of pits or formation of stable pits have been investigated. It was found a number pits initiate well below pitting potential. Out of them only a few may grow to stable , depending on diffusion of ions and formation of porous plug over the pit mouth and other may live for few seconds , called metastable pits and cease to grow further due to favorable condition of repassivation.

Keywords: Metastable pitting; Repassivation; cyclic polarization; Pitting potential; current transient; Electroless Nickel plating;

Introduction

Human tissue may appear to be chemically inert; however, at the molecular level, human tissue is a dynamic environment for immersed metals. Metals implanted into this saline milieu inevitably undergo corrosion, producing detrimental effects both locally and systemically within the human body. The degradation of implanted materials can be brought down to minimum by Passivation. Metals and alloys, such as titanium, cobalt–chromium, and stainless steels, exhibiting passivation have been used as implant materials. Among the metallic materials, AISI 316L stainless steel is most commonly employed for temporary devices such as fracture plates, bone screws

and hip nails due to its low cost and acceptable biocompatibility [1–5]. However, there are many problems related to plate breakage and irritation regarding the fixation devices for osteosynthesis treatment [6–8]. It has been often reported to suffer from severe crevice and galvanic corrosion, primarily due to the presence of occluded sites and high chloride concentration in physiological fluid [9]. The

corrosion of the stainless steel implant releases metal ions such as Fe, Ni and Cr, which produce local systematic effects and thereby plays a role in prosthetic loosening. A study showed that AISI 316L stainless steel produces corrosion products above certain non-lethal concentrations and thereby disturb the proliferation/differentiation relationship of osteoblastic human alveolar bone cell cultures in a dose dependent manner [10].

Extensive research works have been made and still are being carried out to enhance its corrosion resistance and make it more biocompatible. Tomonori Nakanishi and et.al.[11] made solution nitriding of 316L steel and reported to have increased pitting corrosion resistance. acids, bases or combination of them. Various surface modification techniques, such as plasma ion implantation [11–13] laser melting [14–17] and laser surface alloying [18,19] physical and chemical vapor deposition (PVD and CVD)[20,21] thermal oxidation[22] electrochemical surface modification/anodizing [23] have been tried out to improve wear, corrosion, and fretting resistance of orthopaedic implants. However, each of these methods has limitations concerning the performance of tailored surfaces and their complex operating procedures.

Pitting is the most important form of corrosion for austenitic stainless steel in vivo solution. Because growth of it helps to aggravate other forms of corrosion, leading to failure of implant material. Pitting can be mitigated by passivation. Breakdown of passive film leads to initiation of pitting. But all pits, once initiated may not grow. Many of initiated pits are metastable and may be healed by repassivation. Only those of metastable pits which find favorable conditions grow into stable pits [24]. In the present investigation passivation, repassivation and metastable pitting characteristics of 316L stainless steel have been made in Hank solution.

Experimental

316L stainless steel samples of 1X2 cm² were and polished up to 3/0 emery paper, washed with acetone and air-dried by hot air. The samples were observed

with low magnification microscope to find any surface defect of any pit or deep scratch. If any deep scratch or pits were observed, the samples were further polished. This procedure continues until and unless the samples become pit free. Hank solution. was prepared by mixing the analytical grade reagents and double distilled water, with pH value of 7.4 ± 0.2 . Composition of the solutions is listed in table 1. The electrolyte of about 100 ml without aeration was used and temperature maintained at $37 \pm 1^\circ\text{C}$.

Potentiostatic polarization, cyclic polarization and Repassivation experiments were conducted in Gamry instrument. The arrangement electrochemical cell is shown in fig. 1

Results and Discussions

Fig 2 shows the cyclic polarization scan in Hank's solution. The material is found to prone to passivity breakdown and localized corrosion .. The reverse scan cuts the forward scan at 39.71 milivolt vs. SCE which is the Repassivation potential E_{RP} , below which the material is said to be protected against the localized corrosive environment. Since the pitting potential E_{pit} is greater than E_{RP} , localized corrosion initiates and the time of initiation depends on the difference between ($E_{pit} - E_{RP}$). Here E_{pit} is closer to E_{RP} , time of initiation is longer . If E_{pit} is below E_{RP} , localized attack will not continue.

Pits start initiating at certain potentials within passive region. These pits may get repassivated when they are called metastable pits but under certain conditions when the passive force is not enough to cover the exposed local surface area by newly formed oxide layer, the metastable pits grow into stable pits. In the following sets of figures under the study of CPP scan; the aspects of these repassivations have been studied.

In series of experiments from Fig3–6, the specimen is first induced to pit (stimulating phase) by applying a large anodic potential. After pitting has been initiated, the potential is dropped to an already selected test potential to find if the sample is going to repassivate or not. If the specimen repassivates, the process of stimulation and repassivation is repeated at more anodic potential. This technique determines the Critical Repassivation Potential. The experimentation ends during repassivation when the current exceeds the limit indicating of pitting or when the specimen does not pit during stimulation phase. The potential has been stepwise increased within passivity region in Fig. 3 to 6 from the lowest value of -0.085 volt vs. SCE to the highest value of $.121$ volt vs. SCE. In fig. (3), it is seen that repassivation line is absent. At such low potential, pits have not started to initiate

which obviously is an indication to the absence of repassivation line in the respective curve. In fig (4), there is clearly two trends of lines are present; blue line is for stimulation phase and red is for repassivation phase. During this experiment, the potential is raised to -0.07143 volt vs. SCE. It is seen that at such potential, pits have been forced to initiate by the applying current density that is of the order of $.779\mu\text{A}/\text{cm}^2$ and is then dropped to $.2403\mu\text{A}/\text{cm}^2$. The repassivation has simultaneously started with a cathodic current density $-0.529\mu\text{A}/\text{cm}^2$ and the pits have been repassivated. Increase of potential to $.032$ volt vs. SCE shows (Fig 5) a series of lines for stimulation as well as for repassivation phase. When the potential is increased to 0.121 volt vs. SCE (Fig 6), again a series of lines are produced corresponding to stimulation and repassivation phase. For stimulating phase 4 of very high anodic potential, repassivation phase is absent, indicating pits generated have not been repassivated, leading to the formation of stable pits..

For the series of experiments of potentiostatic scan, from Fig 7–13, sample is held at open circuit potential for few seconds and there after it is potentiostated at initial fixed E_{initial} value and is held at this potential for 100 seconds, after which current transit (current vs. time) is studied. Potential is then jumped to E_{final} and is held at that potential and again current transit is studied. Fig (7) shows the potentiostatic scan of the specimen in Hank's solution where the initial potential and final potential has been selected from within the passive region (fig. 2) starting from lower region of the passive curve. It is seen from the current transit study that current steadily decreases with time, indicating no formation of any metastable pits. At higher stepwise potential increase in fig. (8), (9), similar trend of the curve is encountered. From fig. (10) onwards, the trend is a bit different. In fig. (10), it is interesting to find from the second part of the trend that there are several jumps of the current at different time, indicating initiation of pits. But with passage of time, the current density drops down to repassivation and healing of pits starts. This indicates the formation of metastable pits. From fig.(11) and (12), it is quite evident that metastable pits have started to grow into stable pits and therefore repassivation layer is not enough to passivate the deteriorating local passivity layers. Fig (13) shows severe corrosion of the specimen at $.121$ volts vs. SCE.

It is interesting to note from the above discussion that 316L stainless steel in hank's solution does not show any pitting up to $.017$ volt vs. SCE and above it metastable pitting starts while from 0.121 volt vs. SCE stable pits start forming. Fig. (14) shows cyclic polarization curve in Hank's solution of the 316L stainless steel pretreated with high concentration (69%) of nitric acid. If the curve is compared with

the bare sample (fig.2 Cyclic polarization), it is found that there is a drastic improvement in the passivity curve. It has shown positive hysteresis with no indication of localized corrosion.

Electroless nickel deposition in fig. (15) depicts the cyclic polarization curve for the sample pretreated with electroless nickel deposition in Hank's solution. Here again a marked improvement in the passive oxide layer is found. It is also seen that hysteresis loop is totally changed. There is no presence of negative hysteresis loop, indicating high resistive passive oxide layer with very low probability of initiation of pitting. So both the surface treatments have made 316L stainless steel a better corrosion resistant implant material in Hank solution.

Conclusion

The repassivation potential of 316L stainless steel implant in bone solution is 39.71 milivolt vs. SCE which is below pitting potential. So it is prone to localized attack. Metastable pits are generated at potentials within passive region and well below pitting potential. At lower potential less -0.07143 vs. SCE, pits initiate and get passivated, while at higher potential metastable pits grow into stable pits. 316L stainless steel in Bone Fluid Solution, does not exhibit any pitting up to 0.121 volt and above it metastable pits start growing and from 0.121 volt vs. SCE, formation of stable pits start occurring. Surface treatments of the steel with concentrated nitric acid and electroless Nickel plating enhanced corrosion resistance property of the steel. Both the treatments produced positive hysteresis, indicating passivity and absence of localized corrosion.

References

- [1] J. Brunski, in: B. Ratner, A. Hoffman, F. Schoen, J. Lemons (Eds.), Biomaterial Science: An Introduction to Material in Medicine, Academic Press, San Diego, 1996, p. 37.
- [2] M. Sumita, Orthop. Surg. 48 (1997) 927.
- [3] T.P. Ruedi, W.M. Murphy, AO Principles of Fracture Management, first ed., AO Publishing, Davos Platz, 2000, pp. 69–88.
- [4] R.W. Bucholz, J.D. Heckman, C.M. Court–Brown, C.A. Rockwood, D.P. Green, Rockwood and Green's Fracture in Adults, vol. 1, sixth ed., Lippincott Williams & Wilkins, New York, 2002, pp. 181–186.
- [5] H. Hamanaka, Mater. Jpn. 37 (1998) 834–837 (in Japanese).

- [6] R.W. Bucholz, J.D. Heckman, C.M. Court-Brown, C.A. Rockwood, D.P. Green, Rockwood and Green's Fracture in Adults, vol. 2, sixth ed., Lippincott Williams & Wilkins, New York, 2002, pp. 2048–2051.
- [7] E.J. Carragee, J.J. Csongradi, E.E. Bleck, J. Bone Joint Surg. Br. 73 (1991) 79–82.
- [6] J.L. Hughes, H. Weber, H. Wirrenegger, E.H. Kuner, Clin. Orthop. 138 (1979) 111–119.
- [8] U. Lindsjo, Clin. Orthop. 199 (1985) 28–38.
- [9] H. Placko, S. Brown, J. Payer, J. Biomed. Mater. Res. 17 (1983) 655.
- [10] M.A. Costa, M.H. Fernandes, J. Mater. Sci., Mater. Med. 11 (2000) 141.
- [11] Tomonori Nakanishi , Toshihiro Tsuchiyama , Hiromichi Mitsuyasu , Yukihide Iwamoto , Setsuo Takaki , Materials Science and Engineering A 460–461 (2007) 186–194
- [12] P.K. Chu, J.Y. Chen, L.P. Wang, N. Huang, Mater. Sci. Eng., R Rep. 36 (2002) 143.
- [13] S. Mandl, B. Rauschenbach, Surf. Coat. Technol. 156 (2002) 276.
- [14] H. Schmidt, C. Konetschny, U. Fink, Mater. Sci. Technol. 14 (1998) 592.
- [15] H. Badekas, C. Panagopoulos, S. Ecomnomou, J. Mater. Process. Technol. 44 (1994) 54.
- [16] T.M. Yue, J.K. Yu, Z. Mei, H.C. Man, Mater. Lett. 52 (2002) 206
- [17] R. Singh, N.B. Dahotre, Surf. Eng. 21 (2005) 297.
- [18] E. Gyorgy, A. Perez Del Pino, P. Sera, J.L. Merenza, Surf. Coat. Technol. 173 (2003) 265.
- [19] H.C. Man, N.Q. Zhao, Z.D. Cui, Surf. Coat. Technol. 192 (2005) 341.
- [20] A. Matthews, Advances in surface processing technology, in: K.M. Strafford, P.K. Data, J.S. Gray (Eds.), Surface Engineering Practice, Ellis Horwood Ltd, New York, 1990, p. 33.
- [21] C.E. Morosanu, Thin Films by Chemical Vapour Deposition, Elsevier, Amsterdam, 1990, p. 31.
- [22] M.C. Garcia-Alonso, L. Saldana, G. Valles, J.L. Gonzalez-Carrasco, J. Gonzalez-Cabrero, M.E. Martinez, E. Gil-Garay, L. Munuera, Biomaterials 24 (2003) 19.
- [23] B. Yang, M. Uchida, Hyun-Min Kim, X. Zhang, T. Kokubo, Biomaterials 25 (2004) 1003.
- [24] Metastable Pitting Corrosion of Stainless Steel and the Transition to Stability, Pistorius, P. C.; Burstein, G. T., Philosophical Transactions: Physical Sciences and Engineering, Volume 341, Issue 1992, pp. 531–559

Table-1
Composition of Hank Solution

	Concentration (g/L)
Sodium chloride	.8
Calcium chloride	.014
Magnesium chloride	.02
Potassium chloride	.04
Potassium phosphate, mono	.006
Sodium bicarbonate	.035
Sodium phosphate, dibasic	.006
Glucose	.1

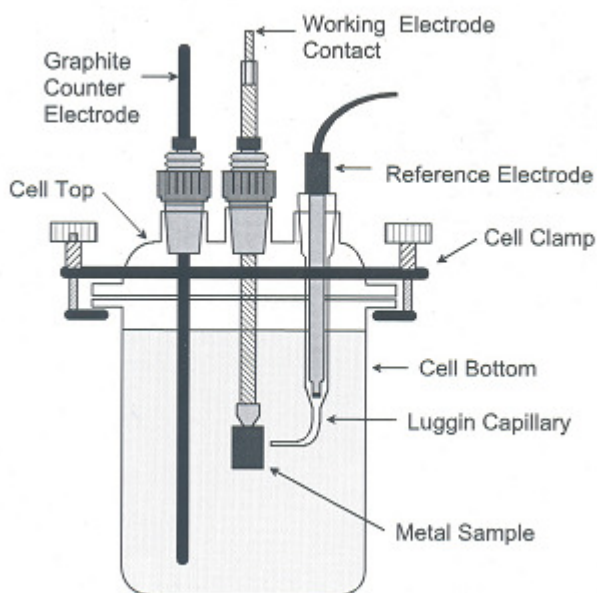


Fig.1 showing experimental electrochemical cell for corrosion study

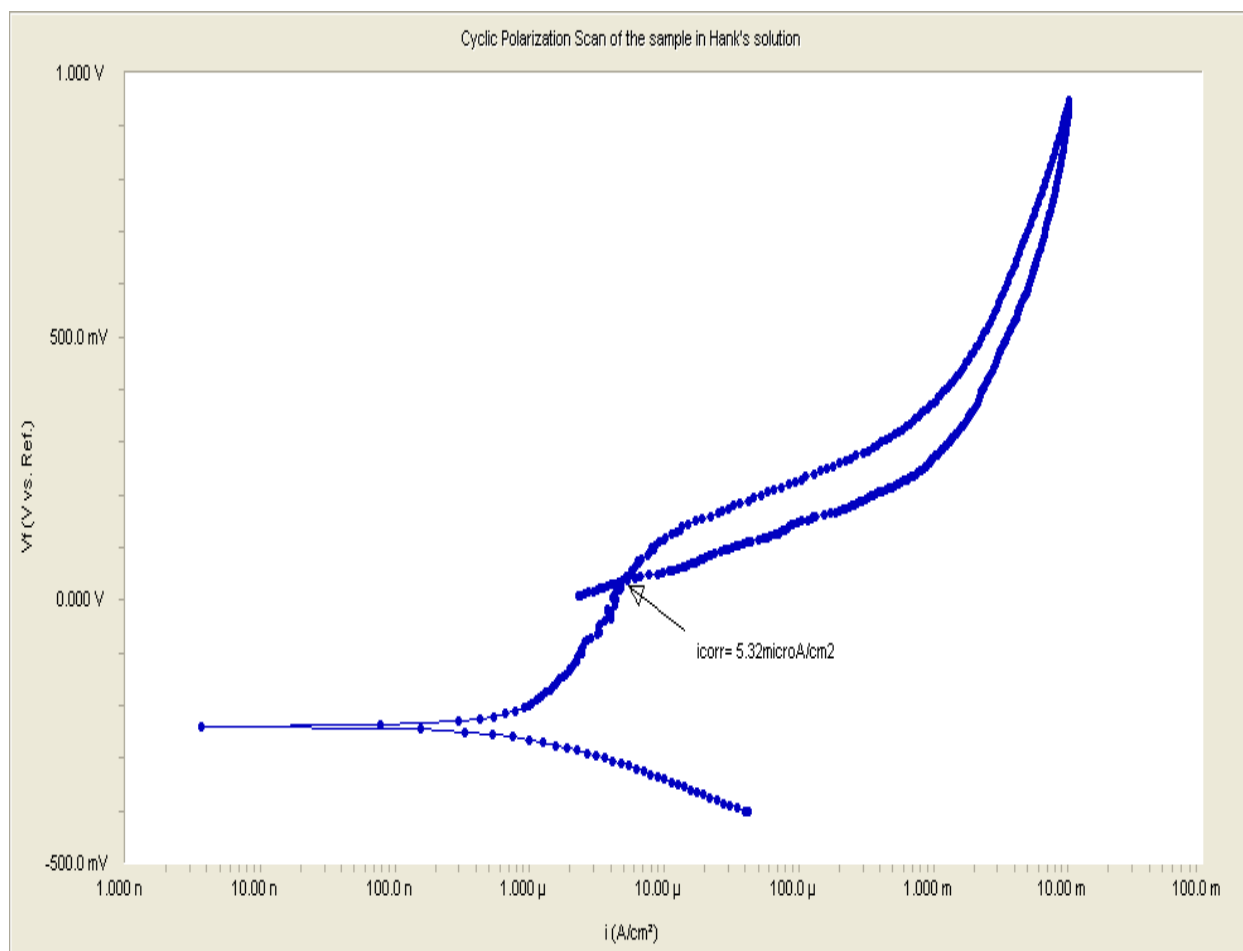


Fig 2: Cyclic Polarization Scan of the Specimen in Hank's Solution

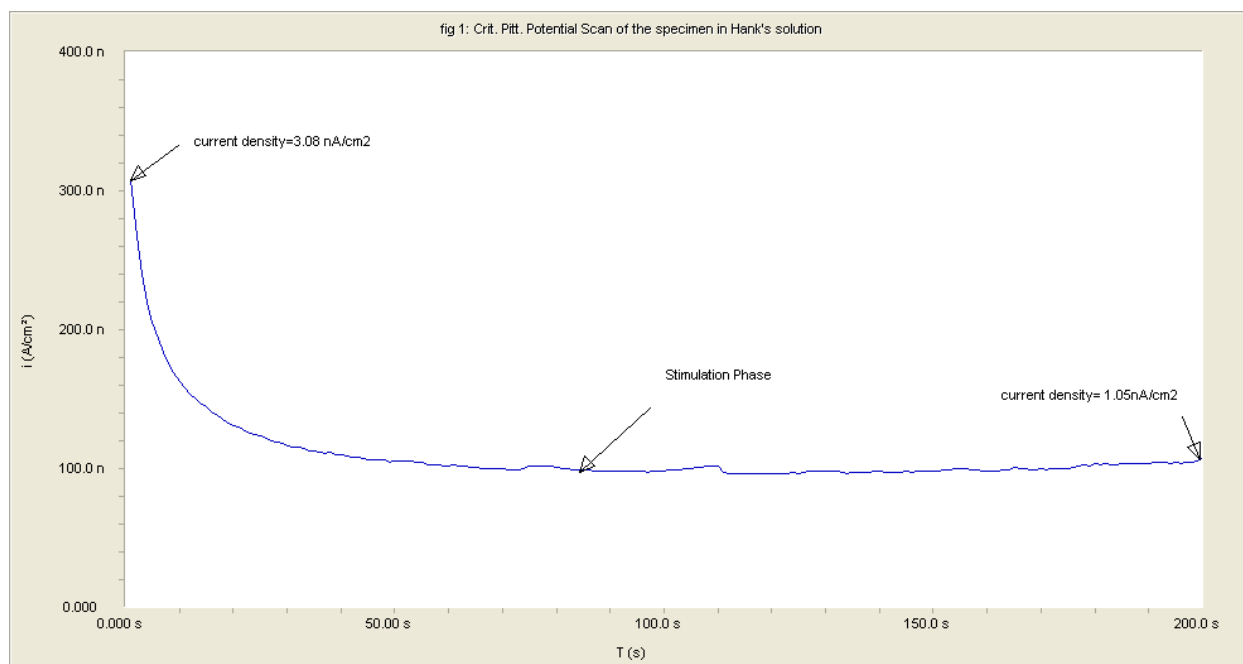


Fig 3: Critical Pitting Potential Scan of the Specimen at -0.085 volt in Hank's Solution

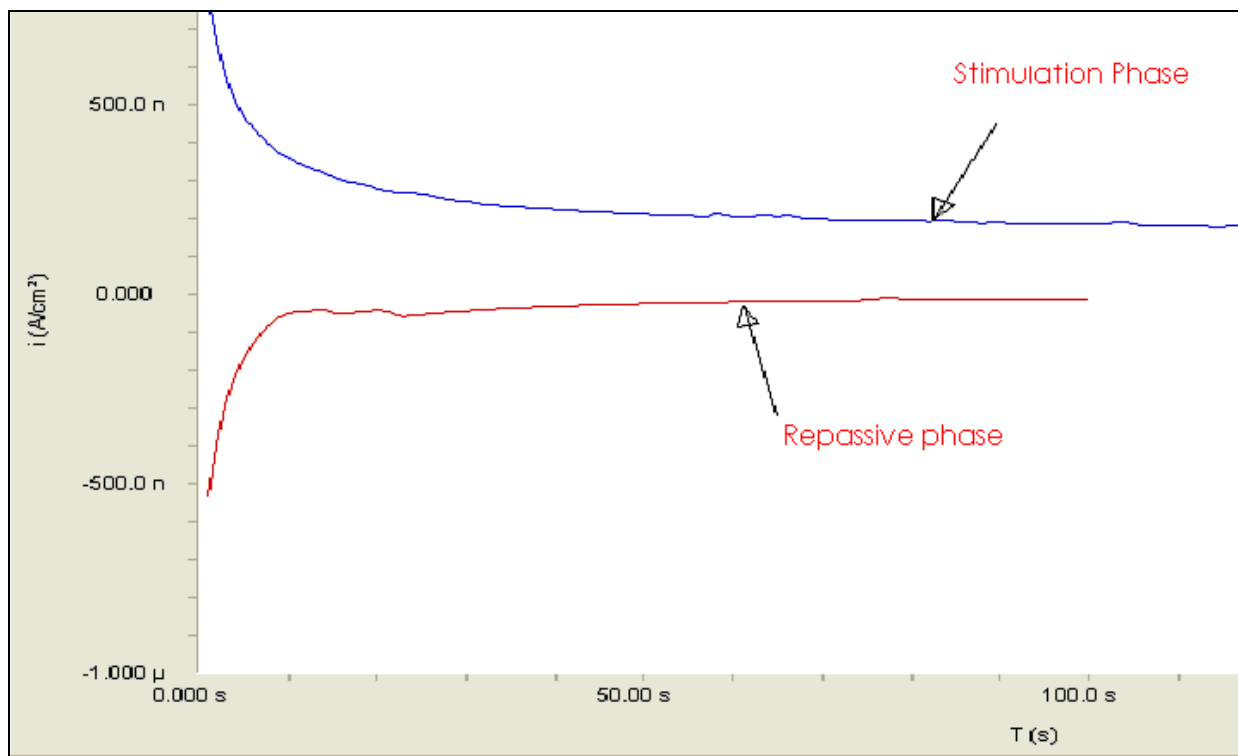


Fig 4: Critical Pitting Potential Scan of the Specimen -0.07143 volt in Hank's Solution

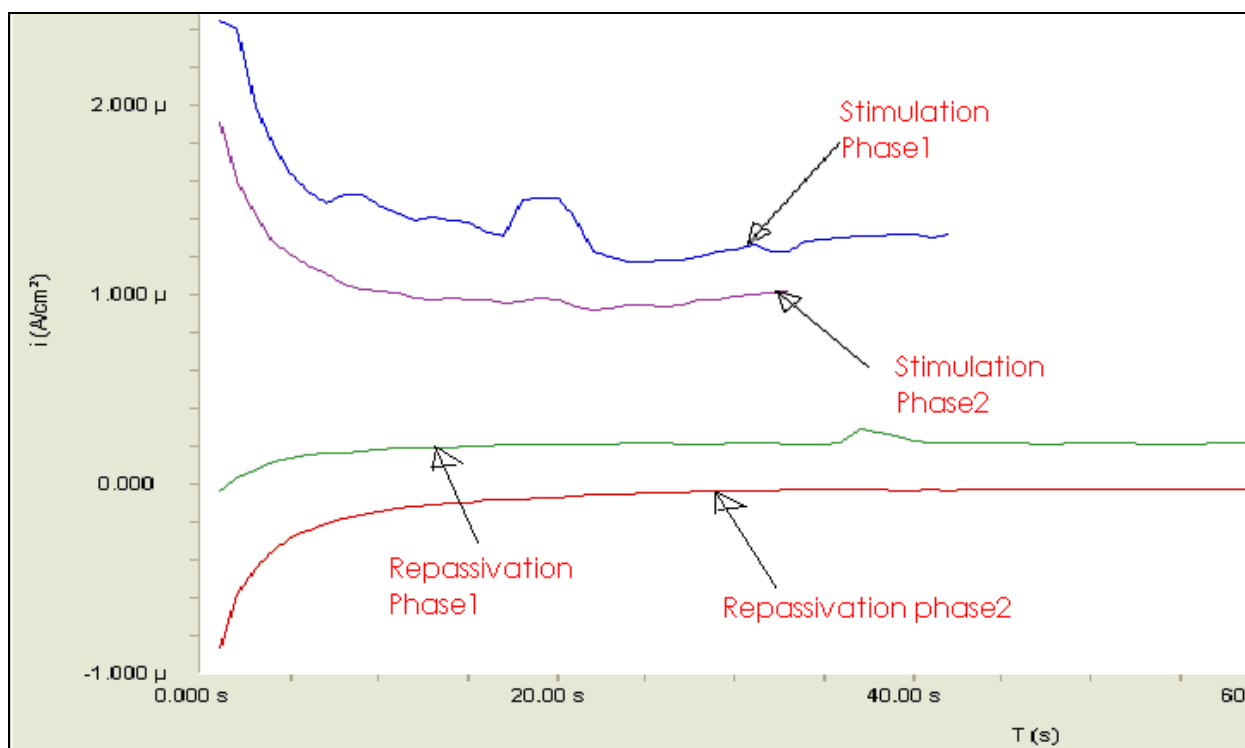


Fig 5: Critical Pitting Potential Scan of the Specimen at 0.032 volt in Hank's Solution

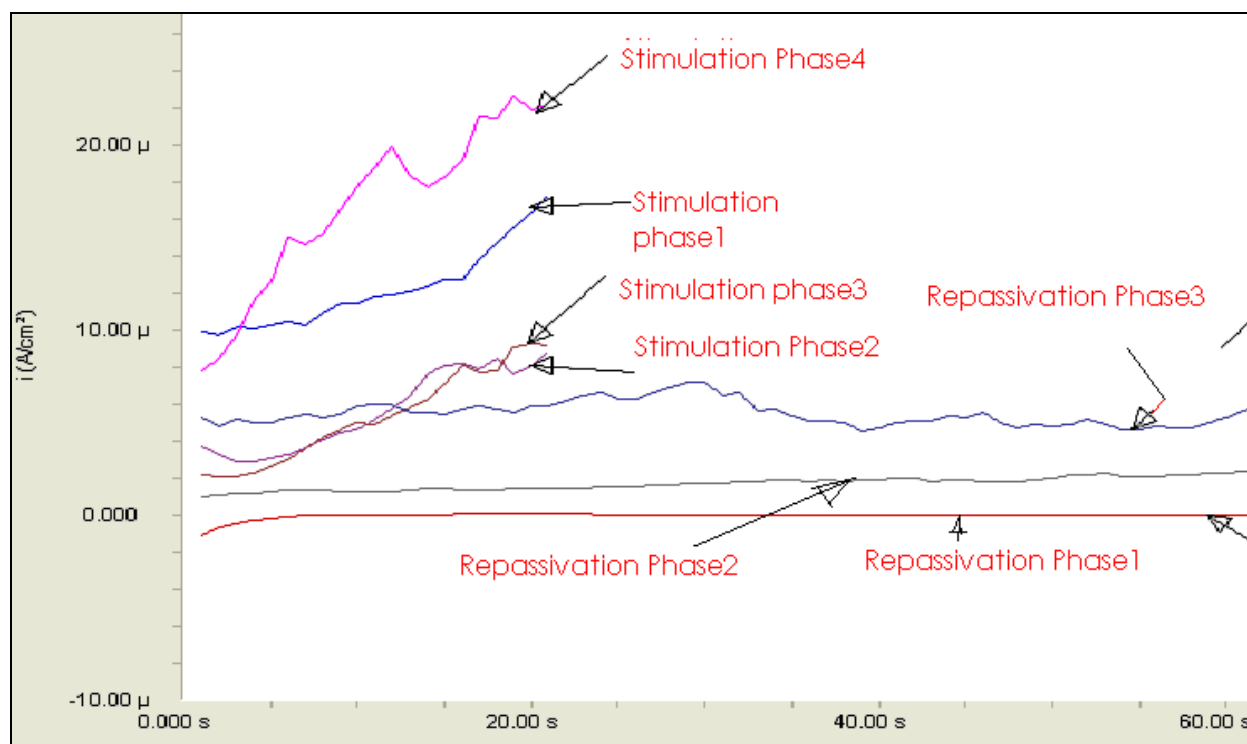


Fig 6: Critical Pitting Potential Scan of the Specimen at 0.121 volt in hank's Solution

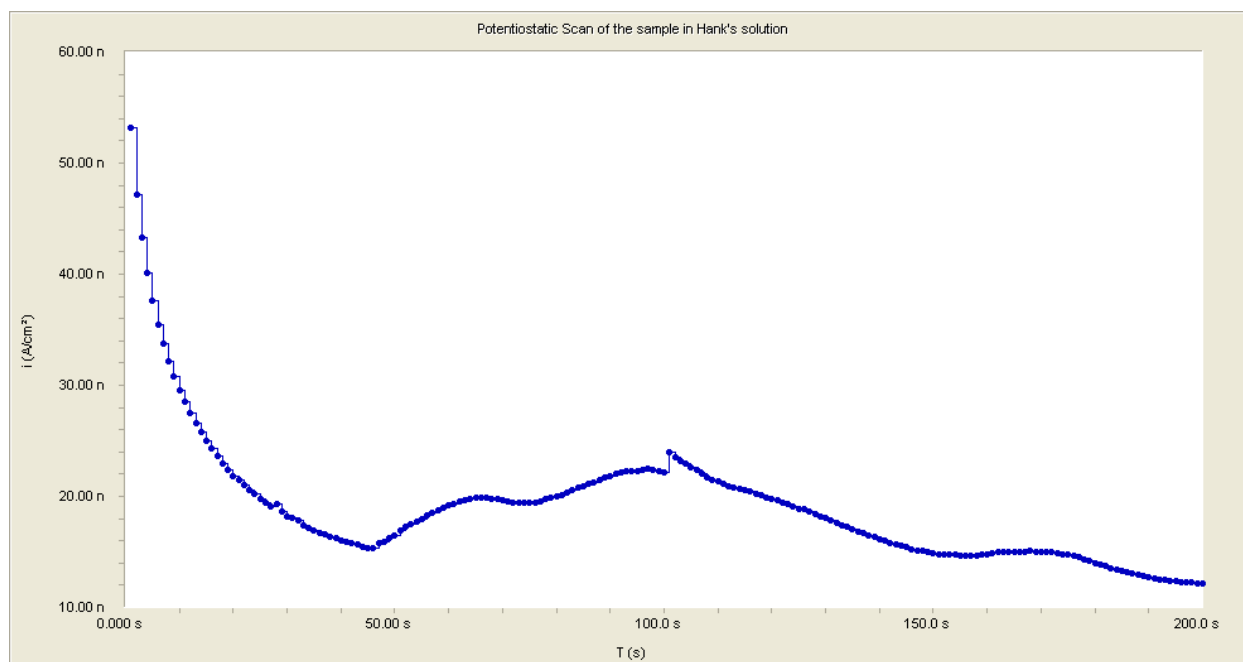


Fig 7: Potentiostatic Scan of the Specimen between -0.085 to -0.071 volts in Hank's Solution

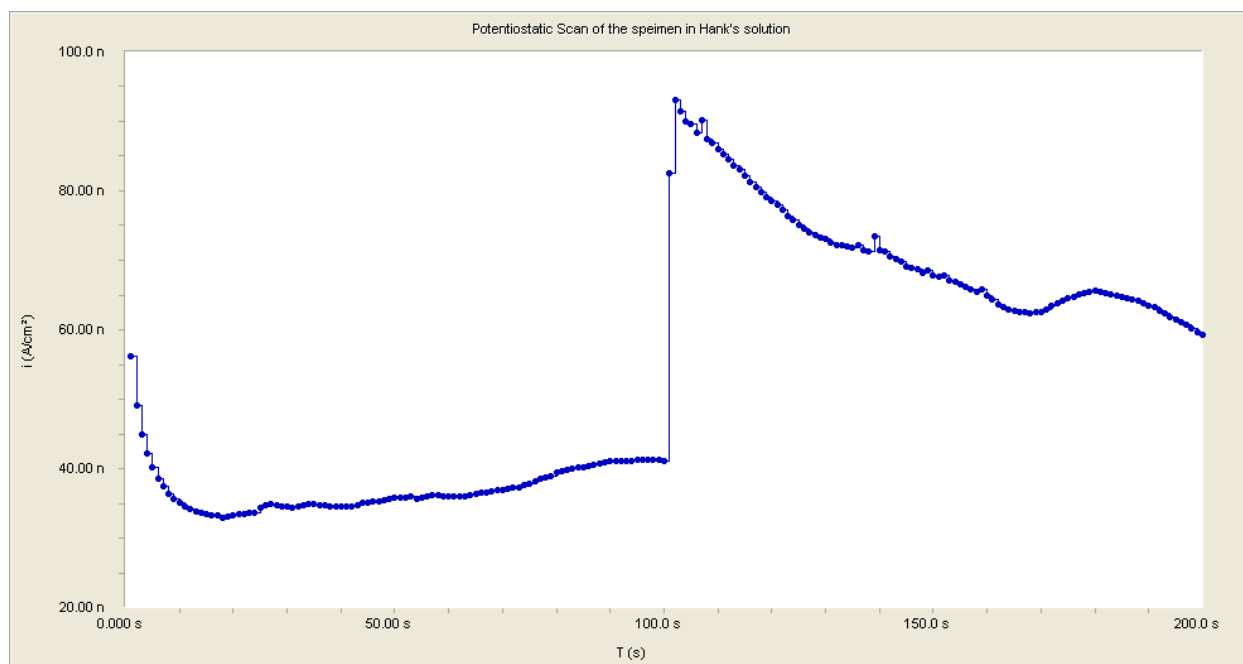


Fig 8: Potentiostatic Scan of the Specimen between -0.071 to -0.017 volts in Hank's Solution

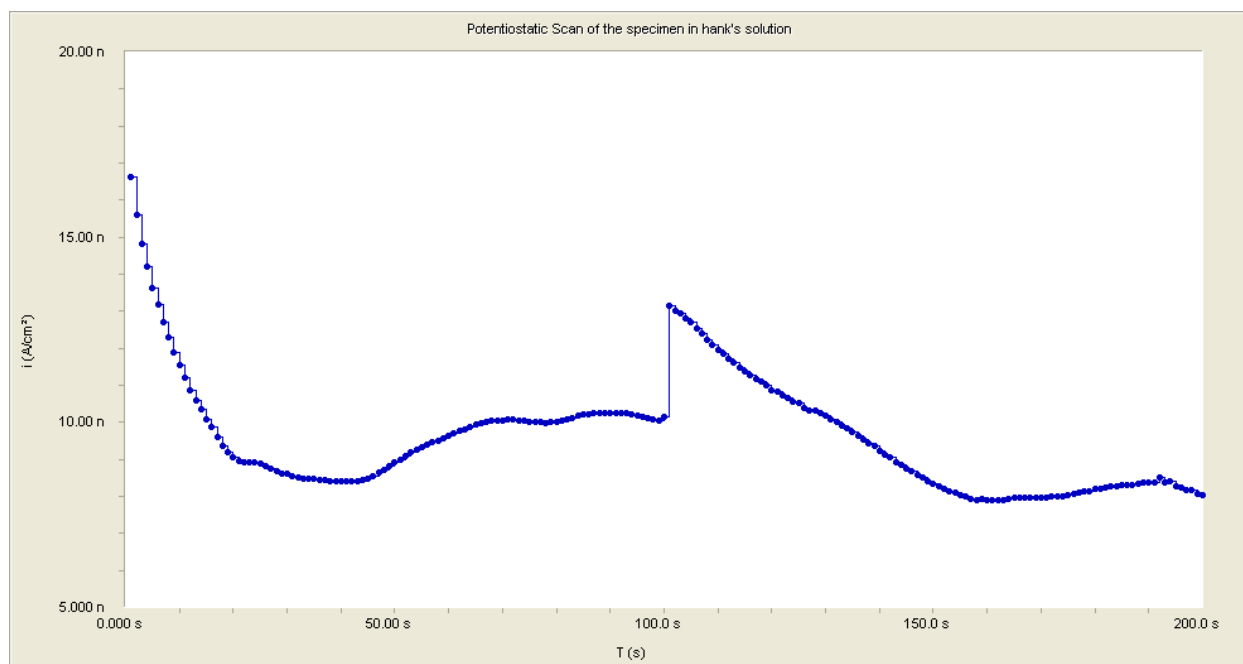


Fig 9: Potentiostatic Scan of the Specimen between -0.017 to 0 volts in Hank's Solution

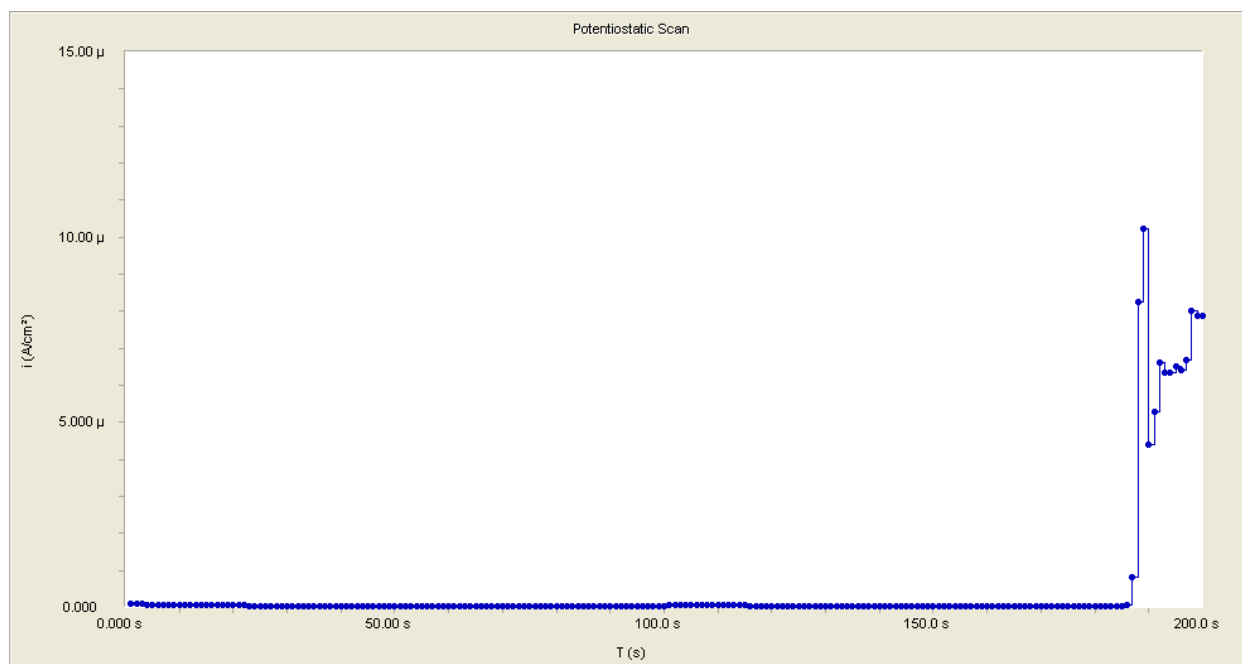


Fig 10: Potentiostatic Scan of the Specimen between 0 to 0.017 volts in Hank's Solution

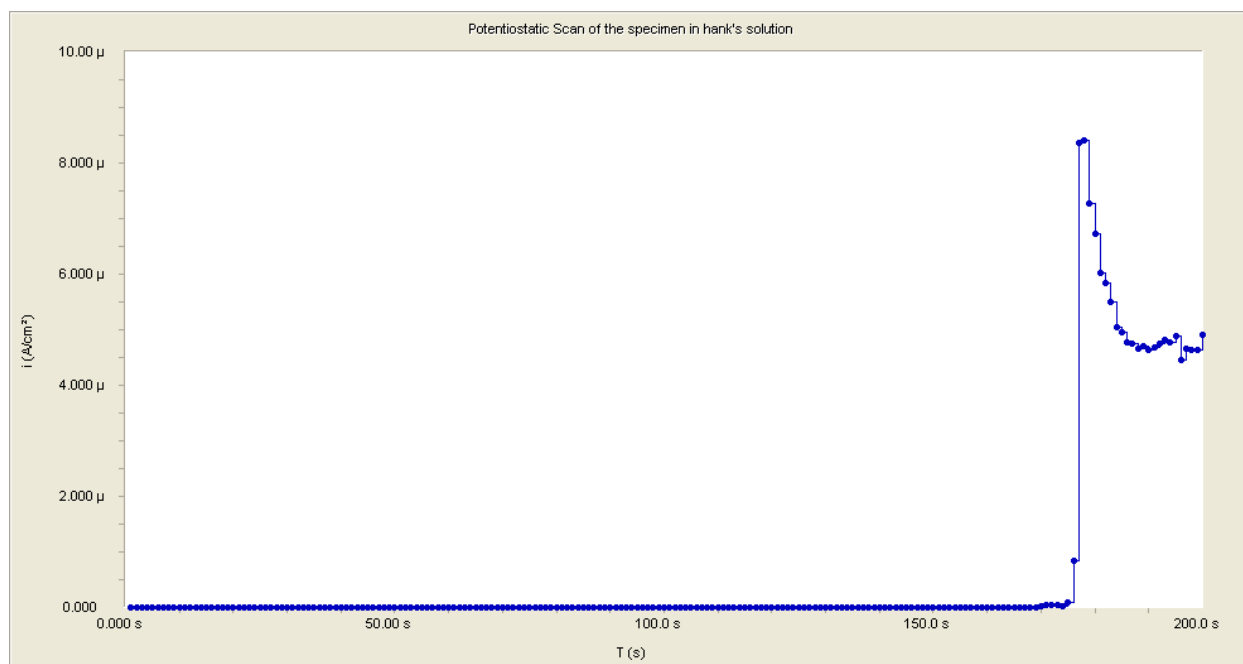


Fig 11: Potentiostatic Scan of the Specimen between 0.017to 0.032 volts in Hank's Solution

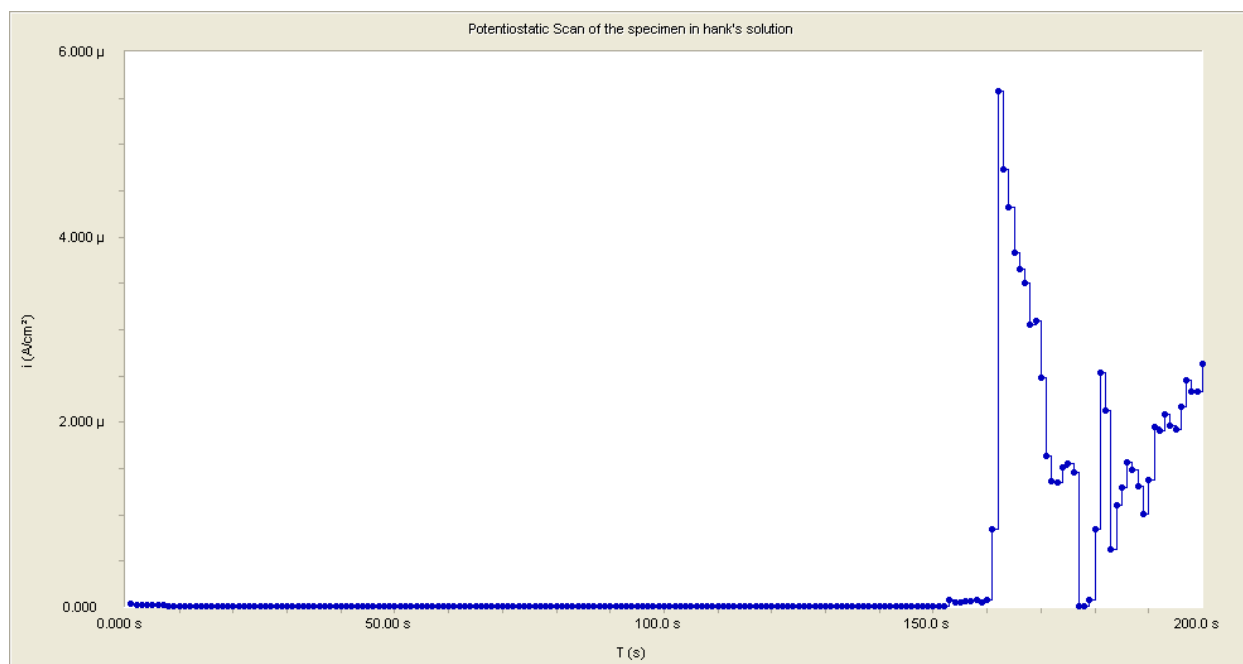


Fig 12: Potentiostatic Scan of the Specimen between 0.032to 0.045 volts in Hank's Solution

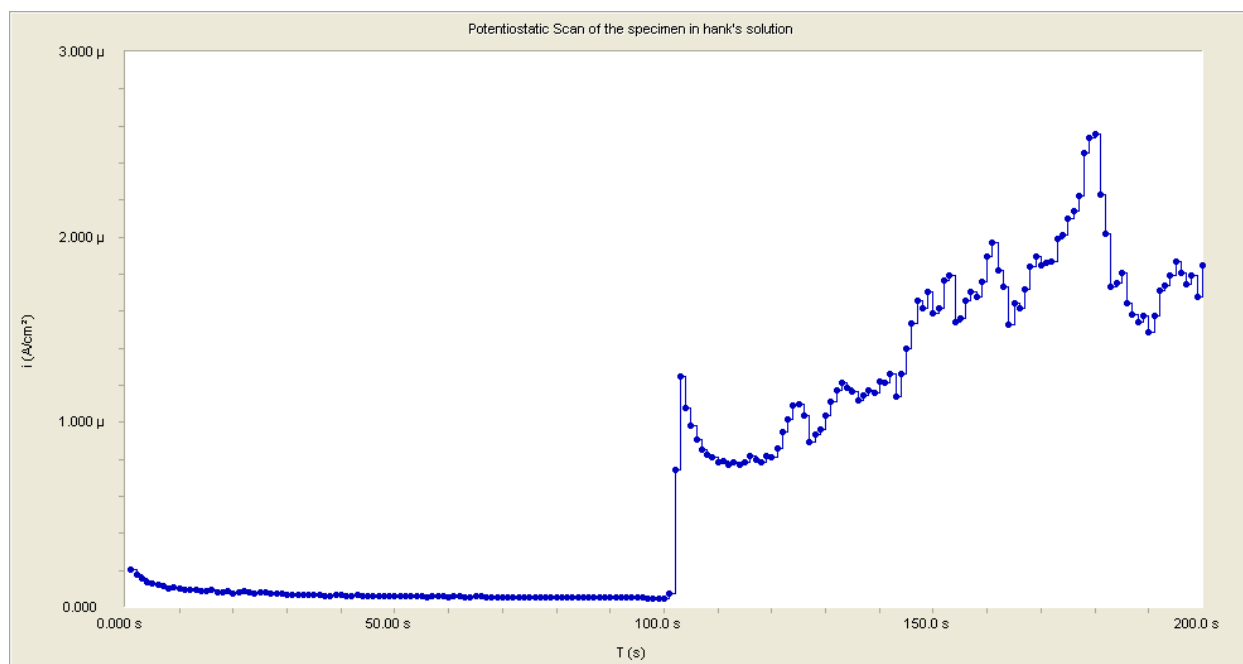


Fig 13: Potentiostatic Scan of the Specimen between 0.045to 0.121 volts in Hank's Solution

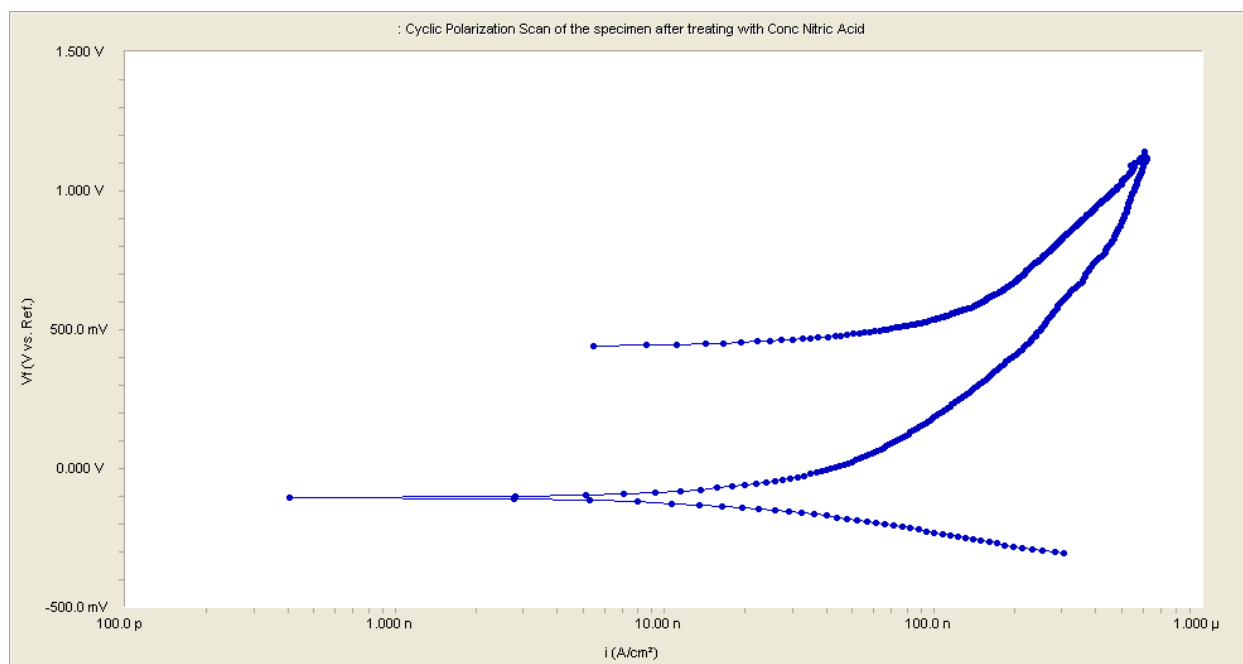


Fig 14: Cyclic polarization scan of the specimen in Hank's solution after treating with 69% nitric acid

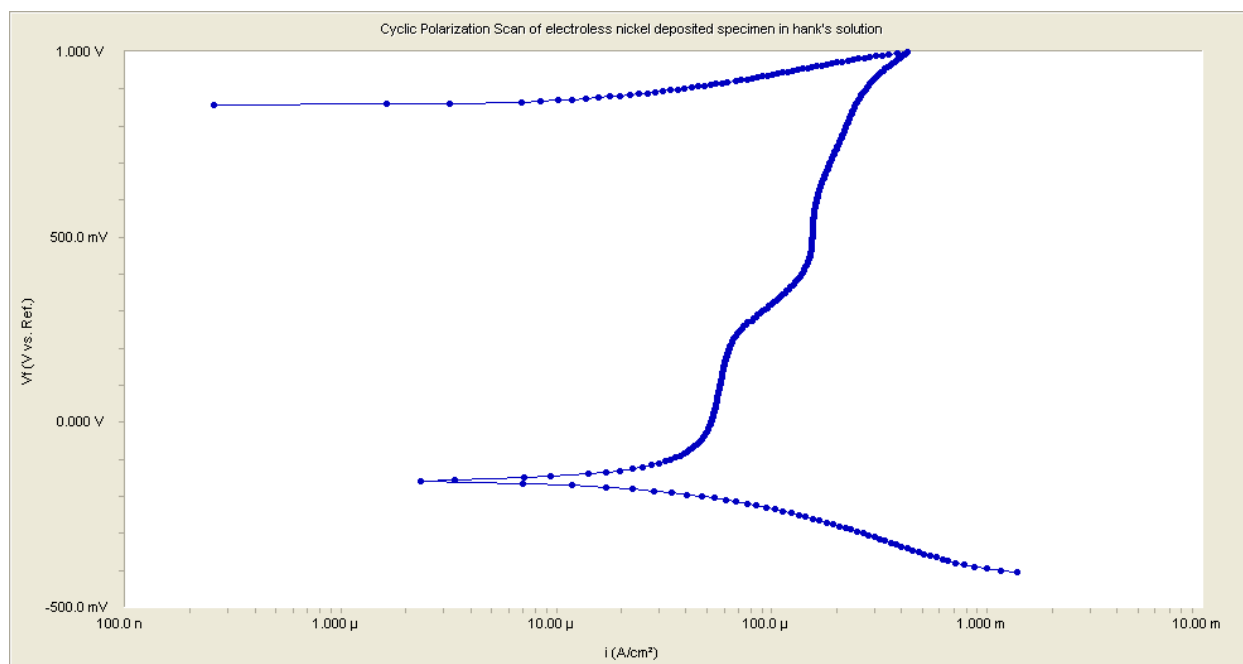


Fig 15: Cyclic polarizations scan of the specimen in Hank's solution after treating with Electroless Ni-deposition